Energy Conversion and Management 256 (2022) 115388

Contents lists available at ScienceDirect

Energy Conversion and Management

journal homepage: www.elsevier.com/locate/enconman

Energy impact evaluation of different low-GWP alternatives to replace R134a in a beverage cooler. Experimental analysis and optimization for the pure refrigerants R152a, R1234yf, R290, R1270, R600a and R744

D. Sánchez *, A. Andreu-Nácher, D. Calleja-Anta, R. Llopis, R. Cabello

Thermal Engineering Group (www.git.uji.es), Mechanical Engineering and Construction Department, Jaume I University, Castellón E-12071, Spain

ARTICLE INFO

Keywords:
R290
R600a
R1270
R152a
R1234yf
R744

ABSTRACT

Due to the entry into force in 2014 of the European F-Gas Regulation n° 517/2014 and the subsequent Kigali amendment, the phase-out of the medium and high-GWP refrigerants has speeded up in all refrigeration fields. The effect on the plug-in or stand-alone systems has meant that other environmentally friendly refrigerants must replace the R134a with low or ultra-low GWP maintaining the same operating conditions and reducing the energy consumption. Extended examples of these fluids are the hydrocarbons R600a and R290 and the inorganic fluid R744 (CO_2). However, there are other alternatives to the HFCs R152a and R1234yf or the hydrocarbon R1270 that have hardly been analysed and can make a positive contribution to this sector. Accordingly, this work aims to evaluate the behaviour of a commercial beverage cooler experimentally when it is optimised with six alternatives to the HFC R134a: R152a, R1234yf, R290, R1270, R600a and R744. Results demonstrated that fluids R290, R1270, R152a, R744 and R600a reduce the energy of R134a in 27.5%, 26.3%, 13.7%, 3.9% and 1.2%, respectively, while the use of R1234yf increases the energy usage to 4.1%.

1. Introduction

The entry into force in 2014 of the European F-Gas Regulation n° 517/2014 caused a considerable stir in the refrigeration and HVAC sector by fixing a preliminary phase-out schedule of high-GWP refrigerants. The main reason to adopt this Regulation was the environmental liability to reduce the Global Warming effect by acting over the direct impact caused by the refrigerant leakages in this sector [19]. Consequently, the refrigeration and HVAC industry had to adapt their equipment to new synthetic or natural refrigerants introducing flammability as a new challenge.

The small-capacity systems typically used in domestic or commercial refrigeration are a clear example of this retrofitting. In Europe, the first units were filled with the CFC R12 and the HCFC R22 until Montreal Protocol come into force in 1987. After that, the HFCs R134a and R404A were used extensively to replace R22 as free ODP refrigerants. However, the adoption of the Kyoto Protocol in 1997 and the came into force of the F-Gas Regulation in 2014 and the Kigali Amendment to the Montreal Protocol in 2019 restricted the use of high-GWP refrigerants and promoted environmentally friendly substances with a very low GWP (below 150) [41,51].

Focusing on commercial refrigeration, plug-in or stand-alone systems are one of the most extended refrigeration systems used to cold down perishable products. According to the International Institute of Refrigeration [26], the equipment used in commercial refrigeration worldwide comprised around 120 million units in 2010, including condensing units, centralised systems and stand-alone machines. The main reason for their extensive utilisation is mainly because of versatility, mobility and relatively low cost. The latter usually makes plug-in systems a gift from product companies to promote its brand or quickly identify its products.

In terms of environmental impact, stand-alone systems have a relatively short life cycle depending on the market trends that affect Global Warming in two different ways: *directly* by the leakages of refrigerant to the environment and *indirectly* by the energy consumption during its operation. From a design point of view, stand-alone systems are endowed with sealed circuits with a refrigerant mass charge between 100 and 400 gr for a cooling capacity of around 500 W [24,48]. However, their average annual leakage ratio can vary extensively from 5 to 12%, depending on the use of the equipment [28,25]

Regarding the indirect emissions, it includes the energy consumption of the whole system that depends on the performance of the refrigeration cycle affected by the refrigerant and the operating conditions

* Corresponding author.
E-mail address: sanchezd@uji.es (D. Sánchez).

https://doi.org/10.1016/j.enconman.2022.115388
Received 25 October 2021; Received in revised form 19 January 2022; Accepted 13 February 2022
Available online 22 February 2022
0196-8904/© 2022 The Authors. Published by Elsevier Ltd. This is an open access article under the CC BY-NC-ND license (http://creativecommons.org/licenses/by-nc-nd/4.0/).

Nomenclature

CFC	chlorofluorocarbon
COP	coefficient of performance
E	energy consumption (kW·h)
GWP	global warming potential
h	specific enthalpy ($kJ \cdot kg^{-1}$)
HCFC	hydrochlorofluorocarbon
HFC	hydrofluorocarbon
HFO	hydrofluoroolefins
RH	relative humidity
HVAC	heating, ventilation, and air conditioning
IHX	internal heat exchanger
LMTD	logarithmic mean temperature difference
$\dot{m}$	mass flow rate ($kg \cdot s^{-1}$)
m	mass (g)
MW	molecular weight ($kg \cdot kmol^{-1}$)
N	rotation speed (rpm)
NBP	normal boiling point (°C)
P	pressure (bar)
PR	pressure ratio
$\dot{Q}$	thermal capacity (W)
SH	useful superheating (K)
SUB	subcooling degree (K)
T	temperature (°C)
t	time (s)
v	specific volume ($m^3 \cdot kg^{-1}$) / volume
VCC	volumetric cooling capacity ($kJ \cdot m^{-3}$)
V_g	compressor swept volume (cm^3)
w	weight
$\dot{W}$	electrical power consumption (W)

Greek Symbols

Δ	variation (increment or decrement)
ε	relative error (%) / thermal effectiveness
λ	latent heat ($kJ \cdot kg^{-1}$)
η_V	volumetric efficiency
η_G	global efficiency

Subscripts

8h or 16h	it refers to the test operating time
air	air
c	compressor
crit	critical
cycle on	it refers to a compressor operation
dis	discharge
end	end
env	environmental
ev	evaporator
gc	gas-cooler
hp	high-pressure side
ihx	internal heat exchanger
in	inlet
ini	initial
iso	isoentropic
k	condenser
lp	Low-pressure side
max	maximum
opt	optimum
out	out / outlet
prod	product
sub	subcooling degree
suc	suction
v	saturated vapour

(ambient temperature, relative humidity or target temperature). Therefore, several authors have analysed different HFC-134a alternatives to enhance the system performance and reduce its environmental impact concerning the refrigerant. These multiple options can be grouped into three categories, including hydrocarbons (R600a, R600, R290 and its mixtures), synthetic substitutes (R152a, R1234yf, R1234ze (E) and its mixtures) and inorganic alternatives as carbon dioxide (R744) [22,32,14].

For **hydrocarbons**, first attempts were introduced in domestic refrigeration to substitute the CFC R12, but in the following years, the target was focused on the HFC R134a. Due to the high flammability of hydrocarbons, a *retro*-fit is mandatory by checking mainly the flammable compatibility of the components and their assembly. From the literature review, most of the studies were carried out by a simple drop-in with a slight *retro*-fit of the capillary tube length. Thus, [1,23] tested a domestic refrigerator with different ternary mixtures of R290, R600 and R600a, proving that they increase the performance of the cycle. Jung et al. [33] analysed theoretically and experimentally an R290/R600a mixture (60/40%w) to replace R12 in two domestic refrigerators. The results proved that using the same hermetic compressor but varying the length of the capillary tube and the refrigerant mass charge, the alternative mixture saves up to 3–4% of energy. Lee and Su [36] tested the R600a with two capillary tubes under different evaporating and condensing levels. The results obtained demonstrated the capability of this refrigerant for domestic applications. Akash and Said (2003) performed several tests to evaluate the convenience of using the mixture R290/R600/R600a (30/55/15%w), resulting in an increment of cooling capacity concerning the R12. Wongwises and Chimres [58] conducted an experimental study to find alternatives to R134a by using binary and ternary mixtures of R290, R600a, R600 and R134a. Taking a R134a household refrigerator as a reference and maintaining the capillary tube and the refrigerant mass charge, they revealed that pure R290 reduces energy consumption up to 27.3% and the mixture of R290/R600 (60/40%w) introduces a saving of 4.2%. Fatouh and El Kafafy [20,21] demonstrated theoretically and experimentally that the mixture R290/commercial butane (60/40%w) could be used as a drop-in for R134a with energy savings of 10.8% at optimised conditions of refrigerant mass charge and capillary tube length. Sattar et al. [54] compared experimentally the energy consumption of an R134a domestic refrigerator using the hydrocarbons R600a and R600. The results showed energy savings up to 3.15% for R600a and 2.44% for R600 without any modification in the refrigerating cycle. Lee et al. [37] tested a small-capacity refrigerator with R134a and the alternative R290/R600a (55/45%w) mixture. After optimising the refrigerant mass charge and the length of the capillary tube, the system reduced the energy consumption to 12.3% with the hydrocarbon mixture. Varying slightly on the composition, Mohanraj et al. [41,42] tested the combination of R290/R600a (45.2/54.8%w) in a domestic refrigerator obtaining energy savings of 11.1% after optimising the length of the capillary tube. A similar analysis was performed by Jwo et al. [34], who tested the mixture of R290/R600a (50/50%w) in a domestic refrigerator designed for R134a without changes achieving energy savings of 4.4% concerning R134a. Rasti et al. [49] conducted an experimental analysis using the refrigerants R600a and R436A (R290/R600a – 54/46%w) to replace R134a in a domestic refrigerator. Maintaining the same R134a compressor, the tests reported 14 and 7% energy savings for R436A and R600a, respectively. However, using a specific compressor for hydrocarbons, the energy savings were 14.6 and 18.7%, respectively. Yu and Teng [60] conducted similar tests but using different proportions for the refrigerant mixture R290/R600a in a single-cabinet refrigerator. From the 24-hour energy consumption tests, the effect of using hydrocarbons instead of R134a reduces the energy consumption up to 29.7% using pure R600a instead of R134a. Sánchez et al. [52] tested the refrigerants R134a, R290 and R600a in a refrigerating plant with the same hermetic compressor under similar operating conditions. Under −10/35 °C evaporating/condensing level, the R290 boosted the cooling capacity and the COP up to 52.7% and 8.8%, respectively, whilst the R600a decreases both parameters 43.4% and 15.9%, respectively.

Regarding the **synthetic solutions**, there are diverse options to replace the HFC R134a, including pure refrigerants and mixtures of them [9,6,45]. Many of these substances allow a direct drop-in or slight retrofit maintaining the same refrigerating circuit. Notwithstanding, most of these substances are flammable, so it is necessary to check the components' explosive compatibility and assembly. To reduce the literature review, we only include those refrigerants with a GWP below 150 according to the limit proposed by the F-Gas regulation. It is worth noticing that this regulation refers to the 4th Assessment Report of the IPCC [29] whilst the 6th Assessment Report has been recently published [31]. Therefore, it is probably that this limit would change in subsequent revisions.

Taking into account the current limit of GWP, Park and Jung [47] evaluated experimentally the refrigerants R134a and R430A (R152a/R600a–76/24%w) in a domestic water purifier at similar operating conditions. With the optimum refrigerant mass charge, the energy consumption of R430A was 13.4% lower than that of R134a. Bolaji [10] tested a refrigerator with refrigerants R134a, R152a and R32. Taking R134a as the baseline, the results showed that R152a was the best option with a maximum energy saving of 4%. Minor et al. [40] experimentally tested three identical beverage coolers optimised for R134a, R1234yf and R744 (CO_2), showing that the HFO R1234yf consumes 0.2% more energy than R134a, while CO_2 reports an increment of 38.2%. Yana Motta et al. [59] conducted an experimental analysis in a small refrigerating system optimised for the refrigerants R134a, R1234yf and R1234ze(E). The authors installed a needle valve to control the useful superheating for the last two fluids, and a 75% larger compressor was used with R1234ze(E). The results advised a COP reduction of around 1% with the R1234yf and about 7% using the R1234ze(E). Karber et al. [35] analysed the experimental performance of a household refrigerator designed for R134a with a direct drop-in with R1234yf and R1234ze(E). Tests revealed that the R1234yf increases the energy consumption by 2.7%, while the R1234ze(E) reduces it by 15.5% with at least 50% more running time. Shapiro [55] tested a commercial bottle cooler with four alternatives to R134a: R1234yf, R1234ze(E), R513A (R1234yf/R134a – 56/44%w) and R450A (R1234ze(E)/R134a – 58/42%w). By using a full pull-down test, the results show energy consumption reductions of 0.0% and 5.2% with R1234yf and R513A, respectively, but an increment of 31.3% and 4.8% with R1234ze(E) and R450A, respectively. Mohanraj [43] presented a theoretical assessment of R430A as an alternative to R134a in a domestic refrigerator. The main conclusions of this study were similar volumetric cooling capacities for both refrigerants and a higher COP for the R430A by about 2.6–7.5% concerning R134a. Cabello et al. [12] conducted tests to compare R134a and R152a in different operating conditions. The results demonstrated that at −10 °C evaporating conditions, R152a is a suitable replacement for R134a with a COP enhancement of 3.4% and a small reduction of the cooling capacity of 3.1%. Aprea et al. [2,3] performed an experimental study where the HFOs R1234yf and R1234ze(E) were used as drop-ins in an R134a domestic refrigerator. Optimising the refrigerant mass charge provided energy savings of 2.6% using the R1234yf and 8.7% for the R1234ze(E). Belman-Flores et al. [7] analysed the energy consumption of a domestic refrigerator designed for R134a when it is refilled with R1234yf without making any modification to the vapour compression system. After a refrigerants mass charge optimisation, the results showed an increment in the energy consumption of about 4% when the HFO R1234yf was used. Sánchez et al. [52] compared experimentally the refrigerants R134a, R1234yf and R1234ze(E) in a small-capacity setup equipped with a hermetic compressor. For the evaporating/condensing level of −10/35 °C, the R152a increases the COP up to 4.8%, whilst the R1234yf and R1234ze(E) decreases the COP 8.3% and 13.0%, respectively, maintaining the same compressor and using an electronic expansion valve. Aprea et al. [4] extended the experimental analysis presented previously, testing two low-GWP mixtures as drop-in of the R134a in a domestic refrigerator. These mixtures with a GWP lower than 150 were R1234yf/R134a (90/10%w) and R1234ze(E)/R134a (90/10%w). The analysis revealed that the mixture of R1234yf/R134a achieves energy savings of around 16.0%, while the mixture of R1234ze(E)/R134a reached 14.1%. Maiorino et al. [39] compared the refrigerants R134a and R152a using a domestic refrigerator as an experimental setup. After a refrigerant mass optimisation to minimise the energy consumption, the study revealed that the R152a allows reducing the energy consumption up to 7.4% concerning the R134a. Bolaji [11] presented a theoretical assessment with five low-GWP zeotropic mixtures to replace R134a. These mixtures were: R440A (R152a/R134a/R290 – 97.8/1.6/0.6%w), R441A (R290/R600/R600a/R170 – 54.8/36.1/6.0/3.1%w), R444A (R1234ze(E)/R32/R152a – 83.0/12.0/5.0%w), R445A (R1234ze(E)/R134a/R744 – 85.0/9.0/6.0%w) and R451A (R1234yf/R134a – 89.8/10.2%w). From the thermodynamic analysis, the refrigerants R440A and R451A showed a COP improvement by 15 and 5%, respectively, with a higher volumetric cooling capacity, around 7 and 4%, respectively. Recently, Morales-Fuentes et al. [44] reported an experimental assessment of a vertical beverage cooler designed for R134a and refilled with R1234yf and R513A. At the ambient temperature of 24 °C, the R1234yf consumes 0.9% lower energy concerning R134a, while R513A reduces the energy consumption up to 3.9%. In all cases, the refrigerant mass charge was fixed to 175 gr.

Finally, concerning the **inorganic alternatives**, the most extended refrigerant as an alternative to R134a is carbon dioxide (CO_2 or R744) due to its non-flammability, non-toxicity, worldwide high availability and environment-friendliness. However, its high pressure and low specific volume do not allow a direct drop-in resulting in a complete system redesign. From the literature, DeAngelis and Hrnjak [16] experimentally test the behaviour of a bottle cooler with R134a as baseline and R744 as an alternative. The results showed that the optimized CO_2 system with a two-stage rolling-piston compressor performs higher COPs than the R134a system equipped with a single-stage reciprocating-piston compressor. Jacob et al. [32] presented an energy comparison between two bottle coolers designed for R134a and CO_2. The first one was equipped with a one-stage rolling piston compressor, and the second one with a two-stage rolling piston. Tests reported two different ambient temperatures where the CO_2 unit had an increment in the energy consumption of 2.2% at 32 °C and a reduction of 8.9% at 24 °C. Rohrer [50] evaluated the energy consumption of a CO_2 bottle cooler equipped with three compressor technologies versus an R134a benchmark system with a single-stage reciprocating compressor. The first technology tested was a rotatory variable speed CO_2 compressor with intercooling between stages that provides 30% energy savings concerning R134a. The second one was a similar compressor but a single speed, saving 15% of electrical energy. Finally, a single-stage reciprocating compressor was tested with energy savings of 17%. Cecchinato and Corradi [15] develop a CO_2 single-door bottle cooler and compare it with an optimized R404A and R134a systems. After optimizing the capillary tube length and the compressor of the CO_2 system, all systems were tested at different ambient conditions maintaining the inner temperature of the cabinet at 5 °C. At the ambient conditions of class 4 (30 °C; 55% relative humidity), the CO_2 unit consumed 54.38% more energy than the R134a unit and 15.89% more than R404A. Elbel et al. [17] and Padilla Fuentes et al. [46] designed and tested a CO_2 glass-door merchandiser system for beverage and refrigerated food with almost similar energy consumption (3% higher) than a conventional R134a system. The design carried out from a low-cost point of view included a redesign of the gas-cooler to minimize the heat conduction, an optimization of the internal heat exchanger to improve its thermal effectiveness, and simultaneous optimization of the refrigerant charge and the capillary tube dimensions. Elbel et al. [18] explored the most relevant design issues for R290, CO_2 and R134a in beverage coolers. They included an experimental comparison among all systems maintaining similar levels of technology and operating conditions. Taking as a benchmark the R134a system, the energy consumption of the R290 system was 9% lower than R134a, while the optimized CO_2 system needed 3% more energy. Regarding the pull-down tests, the optimized CO_2 setup invested the same time as R290, and it was 3% faster than R134a. Finally, Visek et al. [57] evaluated the performance of an R134a beverage dispenser machine when it is upgraded to CO_2. The results from the experimental tests after optimizing the compressor, gas-cooler and the expansion device to achieve an optimal discharge pressure confirmed a notable time reduction in the pull-down process (45% lower) and a slight improvement in the energy consumption (2% lower) at the ambient temperature of 24 °C.

Based on the above, it is evident that there is not a unique solution to replace the refrigerant R134a with other low-GWP substances. Therefore, most of the studies are conducted experimentally, evaluating the performance of a refrigerating unit designed for R134a and retrofitted to a low-GWP solution. However, these studies rarely compare three or more refrigerants using the same refrigerating plant as a test bench, making it difficult to evaluate them. Accordingly, this present work aims to assess the performance of an R134a stand-alone beverage cooler when it is upgraded with different low-GWP alternatives by drop-in (R152a, R1234yf) or by retrofitting (R290, R1270, R600a and R744). For this, the refrigerant mass charge is optimised for each refrigerant to minimise the energy consumption of the setup operating 16 h at the ambient conditions of 30 °C/55% (temperature/relative humidity). Furthermore, a pull-down test was performed to determine the cooling rate of each refrigerant.

2. Theoretical analysis

2.1. Thermodynamic properties of R134a alternatives

Table 1 shows the thermodynamic properties of the analysed R134a alternatives according to the database of RefProp v.10 [38]. In addition, the table includes the ASHRAE safety classification [5] and the value of GWP from the 5th Assessment Report published by the IPCC [30].

2.2. Model description

The thermodynamic analysis has been performed with a computational model of a single-stage vapour compression cycle (Fig. 1) written in MatLab® with the routines of RefProp. This cycle is the most common arrangement used in beverage coolers with the assumptions of adiabatic expansion, no heat transfer to the ambient and a difference of pressure at the compressor discharge and suction port to evaluate the impact on the compressor operation. The operating conditions of the computational model are summarized in Table 2 according to the experimental results of R134a presented in Section 4.

The selected ambient temperature corresponds to a climatic class IV according to the regulation ISO 23953-2. At this condition, we assume

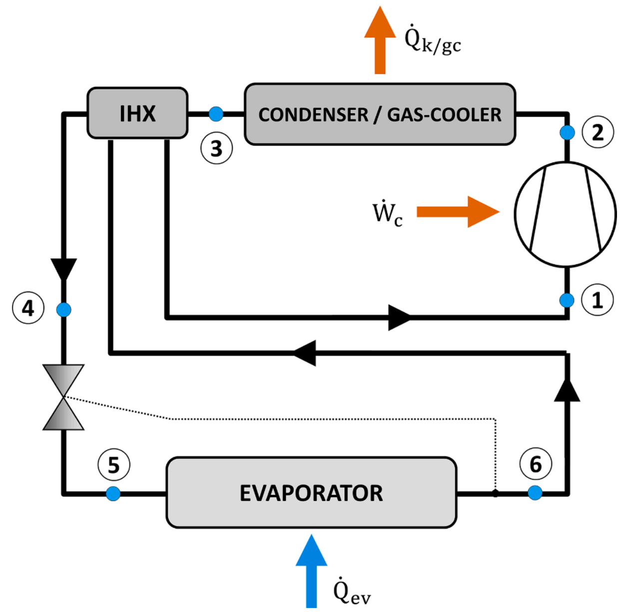

Fig. 1. Schematic diagram of the single-stage vapor compression system.

Table 2
Input data to the computation model.

Variable	Description	Value
T_{ev} (°C)	Evaporation level	−10 °C
SH_{ev} (K)	Useful superheating	6 K
$\dot{Q}_{ev}$	Cooling capacity	390 W
T_{env}	Ambient temperature	30 °C
ΔT_k	Approach temperature in the condenser	4 K
ΔT_{gc}	Approach temperature in the gas-cooler (CO_2)	2.5 K
ΔT_{SUB}	Condenser subcooling degree (excepting CO_2)	3.4 K
N	Compressor rotation speed	2900 rpm
ΔP_{dis}	Overpressure at the compressor discharge	104 kPa
ΔP_{suc}	Pressure drop at the compressor suction	27 kPa
ε_{ihx}	IHX thermal effectiveness	66.4%

that CO_2 operates in a transcritical state; therefore, the heat exchanger that exchanges heat with the ambient changes to a gas-cooler and the subcooling degree at the condenser becomes irrelevant. Either way, the temperature at the condenser or gas-cooler exit (T_3) is obtained from Eq. (1) by adding an approach temperature (ΔT_k or ΔT_{gc}) to the ambient temperature (T_{env}).

$$T_3 = T_{gc\ out} = T_{env} + \Delta T_{gc} \quad \text{for transcritical}$$

$$T_3 = T_{k\ out} = T_{env} + \Delta T_k \quad \text{for subcritical} \tag{1}$$

Excepting CO_2, the condensing temperature (T_k) is calculated with Eq. (2) by adding the condenser subcooling degree (ΔT_{SUB}) to $T_{k\ out}$.

$$T_k = T_{kout} + \Delta T_{SUB} \tag{2}$$

Assuming no pressure drops, the pressure of points 3 and 4 is

Table 1
Thermophysical, environmental and safety characteristics of low-GWP alternatives of R134a.

Fluid	Family	P_{crit} (bar)	T_{crit} (°C)	MW (kg·kmol^{-1})	NBP (°C)	v_v (−10 °C) (m^3·kg^{-1})	λ (−10 °C) (kJ·kg^{-1})	VCC (−10 °C) (kJ·m^{-3})	Safety Group	$GWP_{100\ years}$
R134a	HFC	40.6	101.1	102.0	−26.1	0.0995	206.0	2070.0	A1	1300
R152a	HFC	45.2	113.3	66.1	−24.0	0.1709	317.0	1854.8	A2	138
R1234yf	HFO	33.8	94.7	114.0	−29.5	0.0796	169.5	2128.3	A2L	<1
R600a	HC	36.3	134.7	58.1	−11.8	0.3320	363.5	1094.8	A3	4
R290	HC	42.5	96.7	44.1	−42.1	0.1310	388.3	2963.4	A3	3.3
R1270	HC	45.6	91.1	42.1	−47.6	0.1095	392.2	3582.7	A3	1.8
R744	Inorganic	73.8	31.0	44.1	−56.6	0.0140	258.6	18409.7	A1	1

determined with the condensing temperature at saturated liquid conditions. For the transcritical cycle, the pressure of these points corresponds to the optimal one that maximizes the system COP, which is determined by an iterative process with different pressure values.

$$P_3 = P_4 = P_k = f(T_{k,\ liq\ sat}) \quad \text{for} \quad \text{subcritical}$$
$$P_3 = P_4 = P_{opt} \quad \text{for} \quad \text{transcritical} \tag{3}$$

Pressure at the compressor discharge port (point 2) is obtained taking into account the overpressure fixed in Table 2:

$$P_2 = P_3 + \Delta P_{dis} \tag{4}$$

The evaporating pressure is calculated with the evaporating temperature of Table 2 at the saturated vapour conditions. This pressure is equal in points 5 and 6.

$$P_5 = P_6 = P_{ev} = f\left(T_{ev,\ vap\ sat}\right) \tag{5}$$

The expansion device controls the temperature at the evaporator exit (T_6), and it can be calculated by adding the useful superheating (SH_{ev}) to the evaporating temperature:

$$T_6 = T_{ev} + SH_{ev} \tag{6}$$

Applying the thermal effectiveness definition to IHX and taking into account that the vapour is the fluid with less thermal capacity, the compressor suction temperature (T_1) is defined as:

$$T_1 = T_6 + \varepsilon_{ihx} \bullet (T_3 - T_6) \tag{7}$$

Pressure at the compressor suction port (point 1) is calculated taking into account the pressure drop fixed in Table 2:

$$P_1 = P_6 - \Delta P_{suc} \tag{8}$$

With a simple heat balance in the IHX, the enthalpy at the expansion device inner (h_4) is easily determined with Eq. (9). Considering an adiabatic expansion process, the specific enthalpy h_4 is equal to h_5.

$$h_5 = h_4 = h_3 - (h_1 - h_6) \tag{9}$$

The refrigerant mass flow rate ($\dot{m}$) driven by the compressor is determined with Eq. (10) by a heat balance in the evaporator:

$$\dot{m} = \frac{\dot{Q}_{ev}}{(h_6 - h_5)} \tag{10}$$

The operation of the compressor allows determining its capacity (V_g) Eq. (11), the electrical power consumption ($\dot{W}_C$) Eq. (12) and the discharge temperature (T_{dis}) (Eq. (13)). The model used for this purpose is presented in Equations 13 to 15, with the coefficients gathered in Table 3 [52,53]. We assume the same equations for the refrigerants R290 and R1270 since both refrigerants are very similar [8].

$$\mathbf{V_g} = \frac{\dot{\mathbf{m}} \bullet \mathbf{v}_1}{\eta_V \bullet \mathbf{N}/60} \tag{11}$$

$$\dot{W}_C = \dot{m} \bullet \frac{(h_{2iso} - h_1)}{\eta_G} \tag{12}$$

$$T_{dis} = c_0 + c_1 \bullet P_{suc} + c_2 \bullet P_{dis} + c_3 \bullet T_{suc} \tag{13}$$

$$\eta_V = a_0 + a_1 \bullet P_{suc} + a_2 \bullet P_{dis} + a_3 \bullet T_{suc} \tag{14}$$

$$\eta_G = b_0 + b_1 \bullet P_{suc} + b_2 \bullet P_{dis} + b_3 \bullet T_{suc} \tag{15}$$

Finally, the COP of the refrigerating plant is determined by the Eq. (16) considering the compressor as the unique active element.

$$COP = \frac{\dot{Q}_{ev}}{\dot{W}_C} \tag{16}$$

2.3. Model results

Table 4 gathers the results from the thermodynamic model, including working pressures (P_{ev}, P_k and P_{gc}), pressure ratio (PR), discharge temperature (T_{dis}), power consumption ($\dot{W}_C$), heat rejection ($\dot{Q}_{korgc}$), compressor capacity (V_g), volumetric cooling capacity (VCC), compressor efficiencies (η_G and η_V) and COP.

Analysing the data from Table 4 shows that R744 has the highest working pressure levels with differences of +24.5 bar in evaporation and +71.6 bar during the heat rejection process. Hence, the components for this refrigerant should be robust, particularly at the gas-cooler. Other substances work at similar pressure levels than R134a, excepting R290, R1270 and R600a with differences in the condensing process of +3.4, +6.1 and −4.5 bar with R134a, respectively. The same occurs with the evaporating level, with differences of +1.4, +2.3 and −0.9 bar about R134a. The main effect of these differences affects the pressure ratio and the compressor efficiencies, as Table 2 shown. Considering that the

Table 3
Experimental coefficients for the hermetic compressor.

Volumetric efficiency (η_V)						
Coefficient	R134a	R152a	R1234yf	R290 / R1270	R600a	R744
a_0	0.7247526232	0.7566171921	0.7397796396	0.8245644392	0.7505783148	0.8748614461
a_1	0.0223210176	0.0273964137	0.0110698197	0.0177395862	0.0379972784	0.0046715654
a_2	−0.0099564008	−0.0142596520	−0.0090766299	−0.0112283110	−0.0121273007	−0.0035665060
a_3	0.0019990239	0.0019095772	0.0022774913	0.0017747630	0.0016585362	0.0022098618
ε_{max}	*2.90%*	*2.48%*	*3.74%*	*1.37%*	*6.03%*	*6.50%*
Global efficiency (η_G)						
Coefficient	R134a	R152a	R1234yf	R290 / R1270	R600a	R744
b_0	0.2790630712	0.2754222011	0.2540133488	0.3753611180	0.1777115027	0.5228303246
b_1	−0.0491333270	−0.0434225620	−0.0518935273	−0.0289761062	−0.0422558720	−0.0001637017
b_2	0.0202615201	0.0227531186	0.0231816838	0.0129968640	0.0412987445	−0.0002120453
b_3	0.0020431321	0.0013423916	0.0021953016	0.0010797776	0.0008940846	0.0017040840
ε_{max}	*6.65%*	*8.77%*	*6.82%*	*8.38%*	*9.31%*	*7.30%*
Discharge temperature (T_{dis})						
Coefficient	R134a	R152a	R1234yf	R290 / R1270	R600a	R744
c_0	58.1663247357	59.3293938423	55.8705964667	53.4925077153	48.6855622159	58.2152018056
c_1	−4.5926852516	−4.3423449812	−4.5189435068	−5.6866587361	−5.5200825482	−1.7061220753
c_2	2.7270015964	3.4230299743	2.4847112620	3.0969861813	3.5997761718	0.8771467891
c_3	0.4774887930	0.3346586184	0.4722917510	0.5244999121	0.3504999320	0.6317390785
ε_{max}	*2.38 °C*	*3.04 °C*	*1.78 °C*	*1.99 °C*	*1.58 °C*	*3.66 °C*

Table 4
Results from the theoretical analysis.

Fluid	P_{ev} (bar)	$P_{k\ or\ gc}$ (bar)	PR	T_{dis} (°C)	$\dot{Q}_{k\ or\ gc}$ (W)	$\dot{W}_C$ (W)	V_g (cm^3)	VCC (kJ·m^{-3})	η_G	η_V	COP
R134a	2.0	9.5	6.0	89.0	611.3	221.3	8.85	1299.8	0.450	0.701	1.76
R152a	1.8	8.5	6.1	92.5	613.0	223.0	9.66	1186.4	0.453	0.704	1.75
R1234yf	2.2	9.5	5.4	83.5	614.5	224.5	8.52	1326.6	0.444	0.714	1.74
R600a	1.1	5.0	7.3	73.1	655.6	265.6	17.50	619.4	0.410	0.744	1.47
R290	3.5	12.9	4.4	89.6	588.8	198.8	5.32	1989.1	0.487	0.762	1.96
R1270	4.3	15.5	4.1	93.2	584.5	194.5	4.43	2434.4	0.497	0.747	2.00
R744	26.5	81.1	3.1	98.3	485.2	250.9	1.09	9843.3	0.536	0.749	1.55

global efficiency of the hermetic compressors rarely exceeds 0.6, the discharge temperature will be high (up to 70 °C), and a fan is recommended to cool down the compressor surface. Eq. (13) is determined from a refrigerated compressor with forced airflow.

Regarding the heat rejection, the heat transferred from the condenser/gas-cooler to the environment is on average 593 ± 53 W, which is acceptable for this kind of application. Furthermore, the electrical power consumption of the compressor is around 226 ± 26 W, so no significant changes are required in the electrical components beyond flammable restrictions.

Finally, the differences in COP, volumetric cooling capacity (VCC) and compressor capacity are explained in Fig. 2. The relative COP and the relative volumetric capacity of the alternatives refrigerants are presented about R134a. In this Figure, all the refrigerants above the horizontal dashed line perform a COP lower than R134a, while the refrigerants presented at the right side of the vertical dashed line need a higher compressor capacity than R134a.

According to Fig. 2, R152a and R1234yf have almost the same COP as R134a (lower than 1.4%) but differ in compressor capacities. Thus, for R152a is necessary 9.2% more capacity, while for R1234yf, it falls to 3.7% lower.

Concerning the hydrocarbons R290 and R1270, they perform up to 13.8% better than R134a, and their compressor capacity is, on average, 44.9% lower. Therefore, they need a different compressor adapted for hydrocarbons according to their flammability.

Focusing on R600a, it has the highest specific volume of Table 1, so the compressor capacity is the biggest. Its COP remains the lowest, but its operative pressures are lower than the other alternatives, which minimises the design materials' strength (Table 4). It is worth noticing that R600a is very sensitive to pressure drops, so the pressure introduced to make the analysis could penalise excessively the performance of the cycle.

Finally, R744 (CO_2) performs a COP below all cited refrigerants except R600a. In addition, its highest vapour density entails a reduced compressor capacity, which helps its design for high pressures.

3. Experimental procedure

From the theoretical analysis performed in the section above, the main components' heat transfer processes and the thermal inertia have not been considered. These affect the performance of the cycle, so an experimental analysis is necessary to corroborate the mentioned results. This section describes the testing procedure, including the refrigerating setup, the main changes introduced during the drop-in or retrofit, and the experimental methodology.

3.1. Refrigerating setup

The test bench used in this work consists of a commercial stand-alone beverage cooler with external dimensions 620 (L) × 2000 (H) × 655 (D) mm designed to cool down 460 cans of 330 ml each. The refrigerated unit has a useful inner capacity of 440 L with a glass door at the front to visualize better the products. The cooling unit includes a refrigerating unit with one hermetic compressor (1), two condensers installed in series (2 and 3), one IHX (4), a thermostatic expansion valve (5) and an evaporator (6). Both, evaporator (6) and condenser (3) have axial fans to force the air through them. Fig. 3 presents a simplified schematic diagram of the refrigerating facility, including the main components and measurement elements. Excepting the evaporator, the other components are placed externally at the rear and the bottom of the beverage cooler.

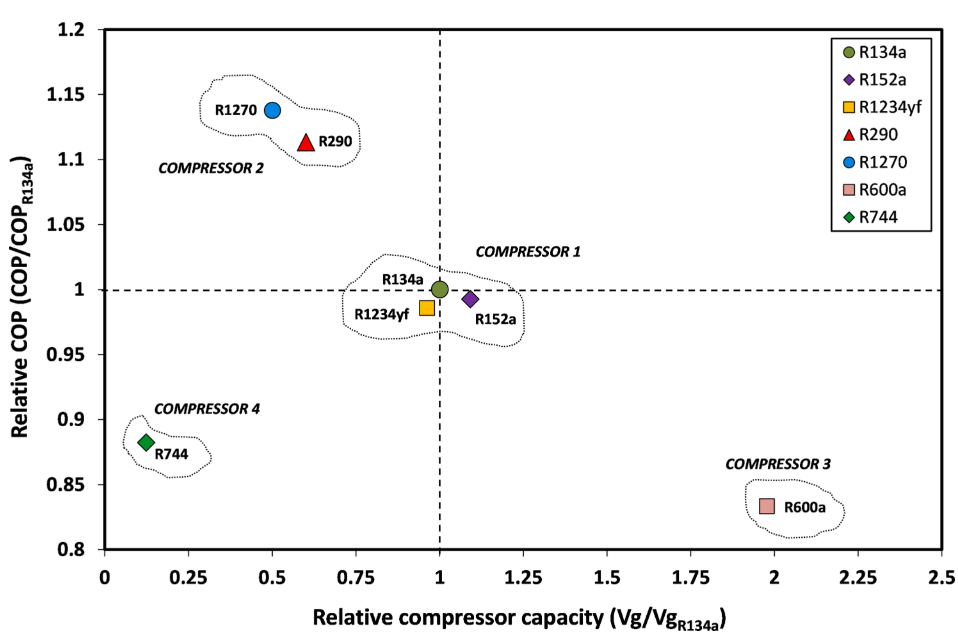

Fig. 2. Schematic diagram of the single-stage vapor compression system.

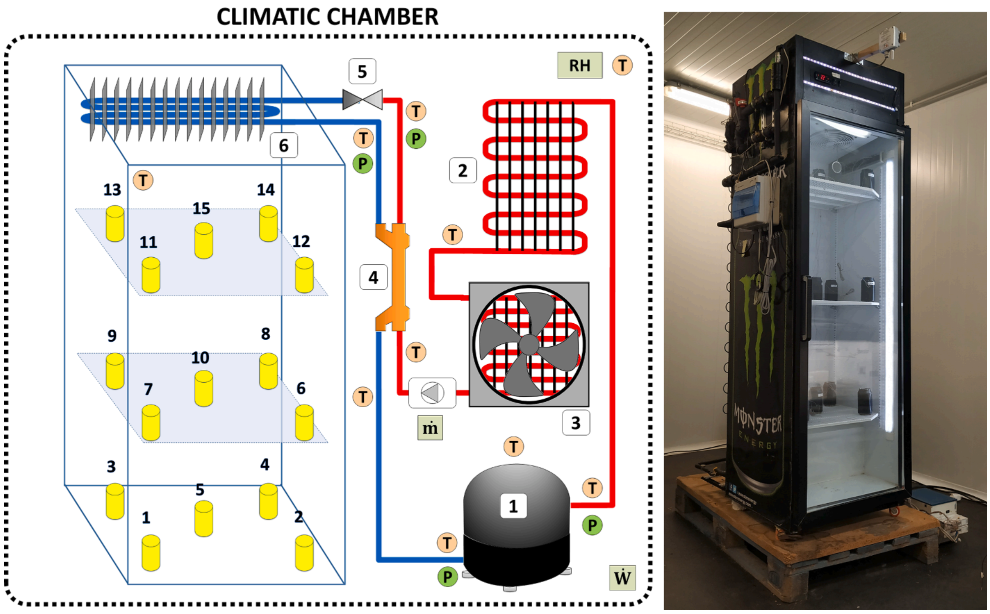

Fig. 3. Schematic diagram of the refrigeration unit (left) and the beverage cooler (right).

All the pipe-lines, excepting the discharge one, are insulated with foam with an average thermal conductivity of 0.036 W·m^{-1}·K^{-1}. Table 5 summarises the main features of these components.

The stand-alone cooler includes a temperature controller with an ON/OFF control system and an adjustable set-point temperature to manage the product temperature. When the inner temperature reaches the set-point configured, the controller switches off the compressor and the axial fans installed in the evaporator (6) and the second condenser (3). Moreover, the controller commands the defrosting process stopping the refrigerating unit every 8 h and waiting for a temperature of 5 °C at the evaporator surface. Usually, the inner temperature is set from 0.9 to 1.1 °C to reach an average product temperature of around 3 °C.

According to Fig. 3, the system is fully instrumented with different measurement elements which main characteristics are gathered in Table 6, including the 15 test cans installed inside the unit to simulate the product (Fig. 3). Although the Fig. 3 does not include the airflow temperature probes, the evaporator includes two thermocouples installed at the airflow inlet and outlet. The digital power meter is installed to measure all the active elements of the beverage cooler, i.e. the temperature controller, two LED lights installed inside and outside the cooler, two axial fans at the evaporator and the second condenser, and the hermetic compressor. The power consumption of the electronic expansion valve and its driver was not included since these systems usually operate with a capillary tube. The use of an electronic valve pursues operating with an optimized expansion system.

Table 5
Principal characteristics of the refrigeration components.

ID	Description	Main characteristics
1	Compressor	Hermetic compressor cooled by air Displacement: see Table 7Nominal rotation speed: 2900 rpm (50 Hz)
2	Condenser	Wire-on-tube heat-exchanger Natural convection Inner heat transfer area: 0.186 m^2
3	Condenser	Finned-tube heat-exchanger Forced convection Heat transfer area: 0.089 m^2
4	IHX	Concentric tube heat-exchanger Heat transfer area: 0.01 m^2 Number of inner tubes: 1
5	Thermostatic valve	Electronic expansion valve
6	Evaporator	Finned-tube heat-exchanger Forced convection Heat transfer area: 0.186 m^2

Table 6
Measurement elements.

Number	Description	Uncertainty, range and features
12	T-thermocouple	±0.5 K Installed over the pipes or elements
2	High pressure Pressure transducer	For CO_2: 0 ÷ 160 bar. ± 0.6% of spam For other: 0 ÷ 16 bar. ± 1.0% of spam
2	Low pressure Pressure transducer	For CO_2: 0 ÷ 60 bar. ± 0.6% of spam For other: 0 ÷ 9 bar. ± 1.0% of spam
1	Relative humidity and temperature transmitter	5 ÷ 98%. ± 2% RH −20 ÷ 80 °C. ± 0.3 °C
1	Power meter	0 ÷ 700 W. ± 0.5% of spam Installed at the power wire of cooler
1	Coriolis mass flow meter	0 ÷ 15 kg·h^{-1}. ± 0.1% of reading Installed at the liquid line
15	330 ml test cans	With an immersion T-thermocouple Mixture of water/propylene-glycol 67/33%v

Finally, data from sensors are gathered by a NI SCXI-1000® DAQ-system every 5 s and stored in a PC for further analysis in MatLab®.

Tests have been performed with different hermetic compressors according to the volumetric cooling capacities described in Table 4 for each refrigerant. However, to minimise the number of compressors and analyse the drop-in effect, we only used four compressors, according to Table 7. The capacity of these was obtained as an average of the theoretical values.

For R600a tests, the compressor used has a capacity lower than the theoretical value because this is the largest compressor commercially available. Notwithstanding, using the technical specifications for this compressor, it can provide more than 390 W at the specified working conditions.

Before testing a new refrigerant, the thermostatic expansion valve was also upgraded for each refrigerant, and the pressure transducers

Table 7
Hermetic compressors specifications.

Refrigerant	Theoretical capacity (cm^3)	Average capacity (cm^3)	Commercial capacity (cm^3)	Characteristics
R134a R152a R1234yf	8.85 9.66 8.52	9.01	9.05	SECOP FR10G Lubricant oil: POE 450 cm^3 2900 rpm (50 Hz)
R290 R1270	5.32 4.43	4.88	4.80	SECOP DLE4.8CN Lubricant oil: POE 221 cm^3 2900 rpm (50 Hz)
R600a	17.50	17.50	14.28	EMBRACO NEK6170Y Lubricant oil: POE 350 cm^3 2900 rpm (50 Hz)
R744 (CO_2)	1.09	1.09	1.10	SANDEM SRFCA Lubricant oil: PAG 200 cm^3 2900 rpm (50 Hz)

were changed in the case of CO_2 due to the high working pressures. However, concerning the other components depicted in Fig. 3, no changes were introduced.

3.2. Methodology

All tests performed with the beverage cooler were conducted at controlled ambient conditions of 30 °C and 55% relative humidity. These conditions correspond to a climatic class IV according to ISO 23953–2:2015, and they are typically used to certify stand-alone systems. The set point established for the average product temperature was around 3 – 3.2 °C on average, with a maximum temperature of 7.2 °C and a minimum above 0 °C [16]. The useful superheating fixed for all fluids were 6 K with a previous upgrading of the electronic expansion valve. Obviously, for each refrigerant, the hermetic compressor was changed according to Table 7.

Concerning the test types, two series of tests were performed for each refrigerant to compare them. The first one, known as the “energy consumption test”, quantifies the amount of energy consumed by the cooler to maintain the product set point temperature during a specific period (usually 24 h). This test is conducted with a particular mass of refrigerant charge that must be optimised to minimise the unit’s energy consumption. Accordingly, the first essays are conducted to find this optimal mass charge for each refrigerant. To reduce the time of experimentation, energy consumption tests were executed for 16 h.

The second test determines the time invested and the energy consumed by the cooler unit to cool down the product from ambient conditions to the desired set point temperature. This test, also known as the “pull-down test”, defines the refrigerant cooling capacity and depends on the initial product temperature and the ability of the refrigerating unit. It is performed with the optimal mass charge, and it usually takes around 8 h.

The test order adopted in the test campaign was: 1st R744, 2nd R134a, 3rd R152a, 4th R1234yf, 5th R290, 6th R1270 and finally, 7th R600a. At each refrigerant, the refrigerant mass charge was first optimised and then, the energy consumption and pull-down tests were performed.

4. Experimental results

This section is divided into two parts devoted to discussing the mass charge optimisation process and analysing the performance of the refrigeration cycle operating at this optimal mass charge. The latter includes operating and energy parameters as phase-change temperatures, heat exchangers operation, power consumption and energy consumption. Furthermore, the pull-down behaviour is also analysed.

4.1. Mass charge optimization

To determine the optimal mass charge, the refrigeration cycle was initially filled with a low refrigerant mass maintaining the reference parameters of product temperature and ambient conditions. After 16 h of operation, the total energy consumption was obtained using the trapezoidal integration method showed in Eq. (16) where “ $\dot{W}$ ” means the electrical power consumed by the beverage cooler (W), “t” is the acquisition time (5 s), and “j” is referred to each measured data.

$$E = \frac{1}{36\cdot 10^5}\cdot\int_0^{16h}\dot{W}(t)\cdot dt \simeq \frac{1}{36\cdot 10^5}\cdot\sum_{j=1}^{16h}\left\{\left[\frac{\dot{W}(j)+\dot{W}(j-1)}{2}\right]\cdot[t(j)-t(j-1)]\right\} \tag{16}$$

Once the energy consumption is known, the refrigeration cycle is charged with an extra refrigerant mass, and the energy test is repeated again. If the new charge reduces the energy consumption, the procedure is repeated until minimum energy consumption is founded. Fig. 4 presents the energy consumption during the optimization process in all tested refrigerants where the optimum mass charge is marked. In total, 70 energy tests were performed during 16 h at the climate conditions of 30 °C and 55%.

Table 8 gathers the main variables of the refrigerating plant at the optimal mass charge, including reference, operating and energy parameters. All the values correspond to average values with the corresponding standard deviation. In the case of the operating parameters, they are evaluated 20 s before the compressor stops.

The optimization process presented in Fig. 4 revealed that almost all low-GWP alternatives could reduce the energy consumption of the R134a configuration excepting the synthetic solution of R1234yf, which increases the energy consumption to + 4.1%.

Regarding the refrigerant mass charge, it depends on the inner volume of the refrigeration cycle, including heat exchangers, pipes and the compressor, which model varies with the refrigerant (Table 7). The optimization confirms that the R744 requires a mass charge of more than twice R134a due to its high density. For the HFO R1234yf and the HFC R152a, the mass increment is 12.0% and 1.7%, respectively, using the same inner volume as R134a. Lastly, the mass charge for hydrocarbons is lower than R134a, with reductions of −43.0% for R290, −47.1% for R1270 and −47.5% for R600a. These charges are lower than 150 g, which are following the restrictions fixed by the current IEC 60335–2 regulation.

4.2. Optimization behaviour

4.2.1. Energy and power consumption

The energy consumption of the refrigeration system considers not only the electrical power consumption of the active elements but also their operating time. This last is presented as the duty-cycle index, defined as the quotient between the time the compressor is ON and the total test time (16 hours). Fig. 5 depicts the energy results calculated with Eq. (16) for each tested refrigerant during 16 h at the optimal mass charge. It is worth saying that this energy consumption is the sum of the energy of all active elements, including the temperature controller and lights (18.4 W), condenser/gas-cooler fan (31.2 W), evaporator fan (30.7 W), and compressor. This last is the most representative element because it represents 68.6 to 76.2% of the total power. Fig. 6 presents the average power consumption of the beverage cooler versus the operating time of the compressor (duty-cycle).

Starting with the synthetic solutions, only the R152a introduces an

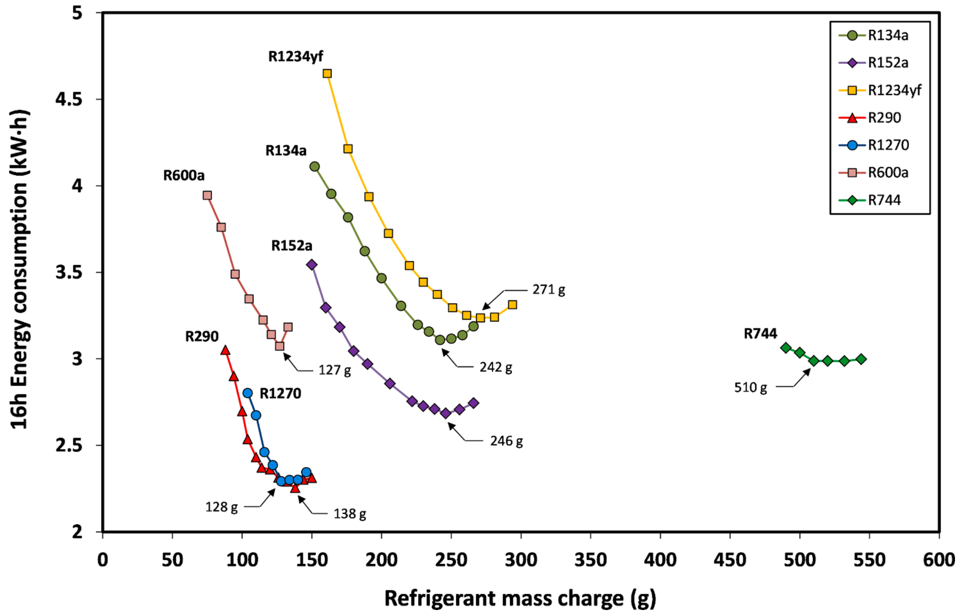

Fig. 4. Refrigerant mass charge optimization.

Table 8
Main parameters of the refrigerating unit at the optimal mass charge.

Refrigerant	m_{opt} (g)	Reference parameters T_{env} (°C)	RH_{env} (%)	T_{prod} (°C)	Operating parameters T_k (°C)	T_{ev} (°C)	T_{dis} (°C)	P_{dis} (bar)	P_{suc} (bar)	Energy parameters $D_{cyle\ ON}$ (%)	$\dot{W}$ (W)	E_{16h} (kW·h)
R134a	242 ± 1	29.8± 0.3	54.5± 2.5	3.1± 0.3	37.4± 0.7	−10.0± 0.5	72.3± 0.6	10.0± 0.2	1.9± 0.1	59.1	311.8± 3.0	3.11
R152a	246± 1	30.1± 0.2	54.1± 1.2	3.1± 0.3	37.2± 0.9	−8.5± 0.9	67.3± 2.9	8.9± 0.2	1.8± 0.1	51.5	307.9± 4.3	2.68
R1234yf	271± 1	29.9± 0.1	55.2± 0.4	3.1± 0.3	44.7± 0.3	−11.7± 1.4	72.3 ± 1.1	12.0 ± 0.1	1.9 ± 0.1	61.6	307.8 ± 7.4	3.24
R290	138 ± 1	29.7 ± 0.2	55.2 ± 1.0	3.1 ± 0.3	39.5 ± 0.3	−10.2 ± 1.3	54.6 ± 1.2	13.8 ± 0.1	3.4 ± 0.1	50.7	255.9 ± 2.8	2.25
R1270	128 ± 1	30.1 ± 0.3	55.1 ± 1.2	3.2 ± 0.3	37.0 ± 0.3	−11.3 ± 1.4	66.5 ± 1.1	15.2 ± 0.2	4.1 ± 0.2	47.8	277.4 ± 3.4	2.29
R600a	127 ± 1	29.8 ± 0.1	53.4 ± 0.2	3.2 ± 0.4	37.7 ± 0.2	−9.4 ± 0.5	72.3 ± 0.9	5.4 ± 0.0	1.0 ± 0.0	67.3	274.0 ± 2.6	3.07
R744 (CO_2)	510 ± 1	30.1 ± 0.5	53.8 ± 3.7	3.2 ± 0.4	–	−7.8 ± 0.8	77.2 ± 2.7	80.6 ± 1.3	28.2 ± 0.7	55.8	337.7 ± 3.5	2.99

energy saving of −13.7%, whilst the R1234yf increases the energy consumption to +4.1%. This behaviour is a consequence of the compressor duty cycle, as reflected in Fig. 6. The R1234yf has similar average power consumption to R134a, but it makes longer the compressor operation resulting in an increment of energy consumption. For the R152a, the effect is just the opposite, it consumes in similar average power, but it has a −12.9% lower duty-cycle than R134a. This behaviour means that the R152a is able to produce a higher cooling capacity than R1234yf.

The hydrocarbons report energy savings of −27.5% for R290, −26.3% for R1270 and −1.2% for R600a. The main reason for R290 and R1270 is the reduction in power consumption and compressor duty-cycle, as depicted in Fig. 6. In the case of R600a, this reduction is a consequence of the minimization of power consumption since the compressor duty-cycle is + 13.9% higher than R134a.

Finally, the use of R744 at the optimal operation conditions reduces the energy consumption up to −3.9% due to the lower running time of the compressor (−5.6% regarding R134a) despite its higher power consumption compared with R134a.

4.2.2. Operating temperatures

The representative temperatures used to compare all refrigerants are discharge temperature, condensing temperature and evaporating temperature. The phase change temperatures presented in Fig. 7 are evaluated with the average pressure at the condenser and evaporator, assuming saturated liquid for the condensing level and saturated vapour for the evaporating temperature. For CO_2, the cycle operates in transcritical conditions, so the temperature shown in Fig. 7 corresponds to the exit of the gas-cooler.

The compressor discharge temperatures in Fig. 8 were measured directly by a thermocouple insulated thermally and installed 10 cm after the compressor. In all cases, temperatures are evaluated as an average of 20 s before the compressor stops.

From Fig. 7, it can be observed that almost of refrigerants present similar condensing temperatures to R134a excepting R1234yf and the R744, which temperatures are + 7.33 K higher and −5.52 K lower than R134a, respectively. In the first case, the increase is related to the low heat transfer performance of R1234yf during the condensing process compared to R134a [27]. In the last case, the transcritical operation of R744 allows operating near the heat rejection temperature due to the high thermal efficiency of the gas-cooler [13,56]. As a result, the gas-

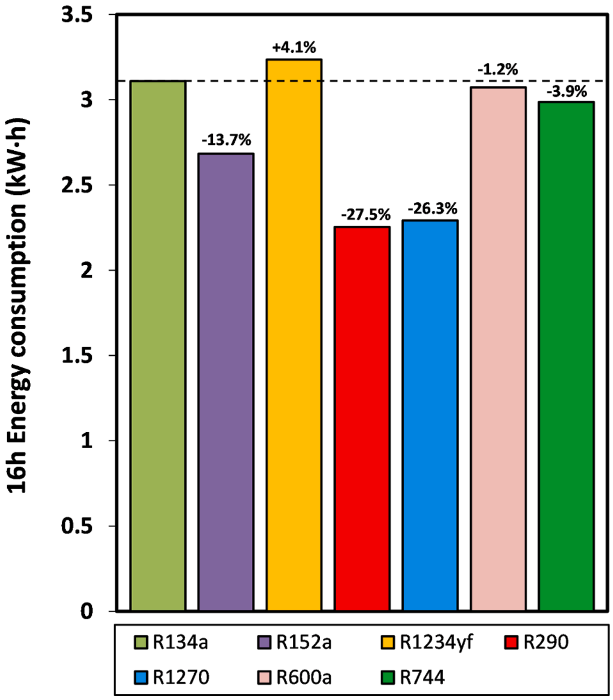

Fig. 5. Energy consumption during 16 h.

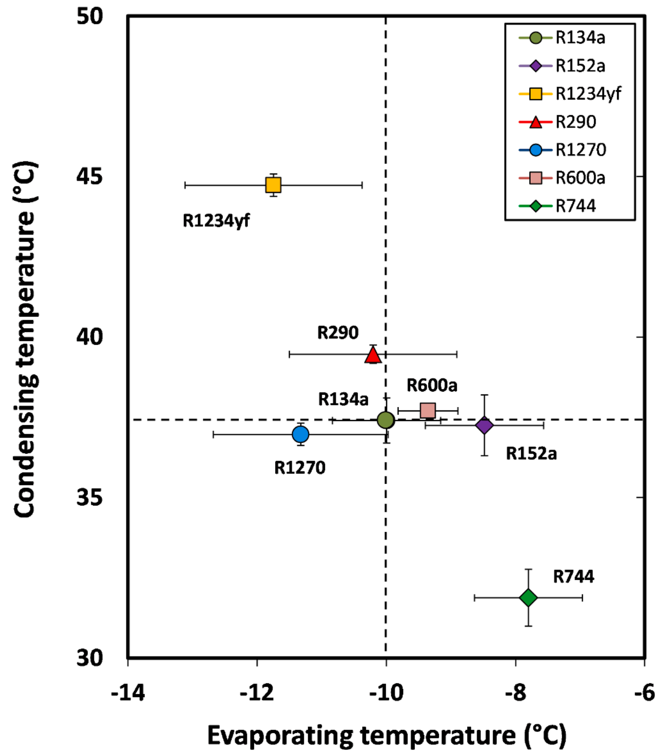

Fig. 7. Average phase-change temperatures (T_{env}:30 °C).

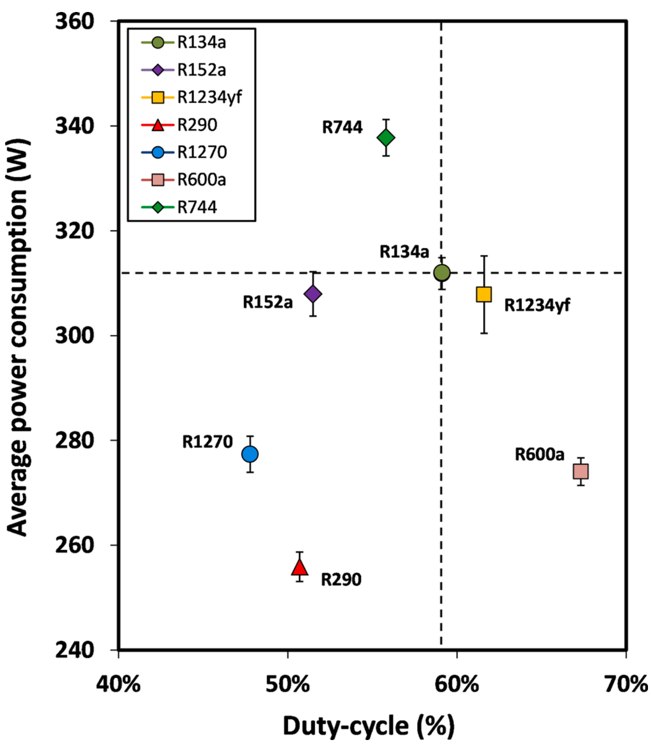

Fig. 6. Average power consumption vs. duty-cycle during 16 h.

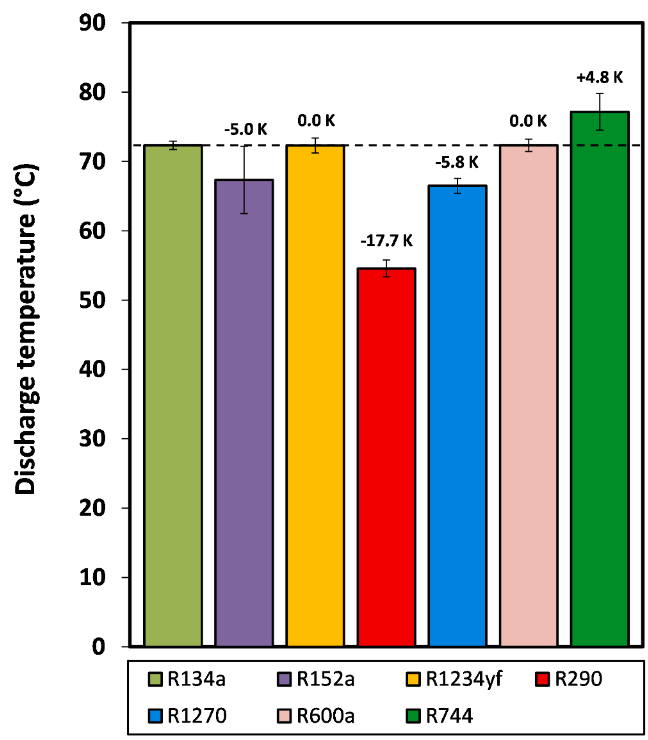

Fig. 8. Average compressor discharge temperature.

cooler approach temperature reaches 1.79 K concerning the ambient temperature.

Regarding the evaporating temperature, the behaviour is similar to the condensing one. The refrigerants with evaporating temperatures lower than R134a are R1270 and R1234yf, with decrements of −1.33 K and −1.75 K, respectively, whilst the refrigerants R152a and R744 perform higher evaporating temperatures than R134a: +1.51 K and +2.19 K, respectively. The main consequence is that the evaporator's performance improves when used with refrigerants R152a and R744 and worsens with R1234yf.

Finally, the discharge temperature presented in Fig. 8 reveals that the HFO R1234yf and the hydrocarbon R600a have similar discharge temperatures to R134a, while the fluids R152a, R290 and R1270 decrease this value to −5.0 K, −17.7 K and −5.8 K, respectively. For

R744, the discharge temperature increases slightly to +4.8 K, so we can affirm that no significant differences are found in discharge temperature.

4.2.3. Operating pressures

The pressure indicators summarized in Table 8 represent the compressor's discharge and suction pressure because they are the highest and the lowest pressure levels in the refrigerating cycle. Fig. 9 depicts the average values of both, where it is evident that the R744 has the most significant pressures due to its high density. Notwithstanding, focusing on the other refrigerants, it is remarkable that all fluorinated alternatives have similar evaporating levels with a slight increment of 1.5 bar on average, above and below the condensing pressure of the R134a. Furthermore, the hydrocarbons R290 and R1270 always perform with pressure levels higher than the R134a being the R1270, the fluid with the most significant increment. Finally, R600a pressures are below the R134a levels, and the evaporating pressure is similar to atmospheric pressure, reducing pressure design requirements in the heat exchangers.

Regarding the pressure ratio, the average values presented in Fig. 10 define the quotient between the discharge pressure and the suction pressure at the compressor. As shown, the refrigerants R1234yf and R600a demand higher pressure ratios whilst the other fluids operate with lower values than R134a. Worthy of special mention has carbon dioxide (R744), which reduces 46.5% on average the R134a pressure ratio. These values affect the compressor efficiencies and, consequently, the mass flow rate, so that the lower the pressure ratio, the better the efficiencies and the mass flow rate are.

4.2.4. Heat exchangers operation

The evaluation of the heat exchanger operation helps to determine its good performance using a specific refrigerant. In this case, the evaporator and the internal heat exchanger (IHX) have been evaluated using the parameters of thermal efficiency (ε), subcooling degree (SUB) and logarithmic mean temperature difference (LMTD). Eqs. (17) to (20) were used to determine these values. The vapour is assumed as the

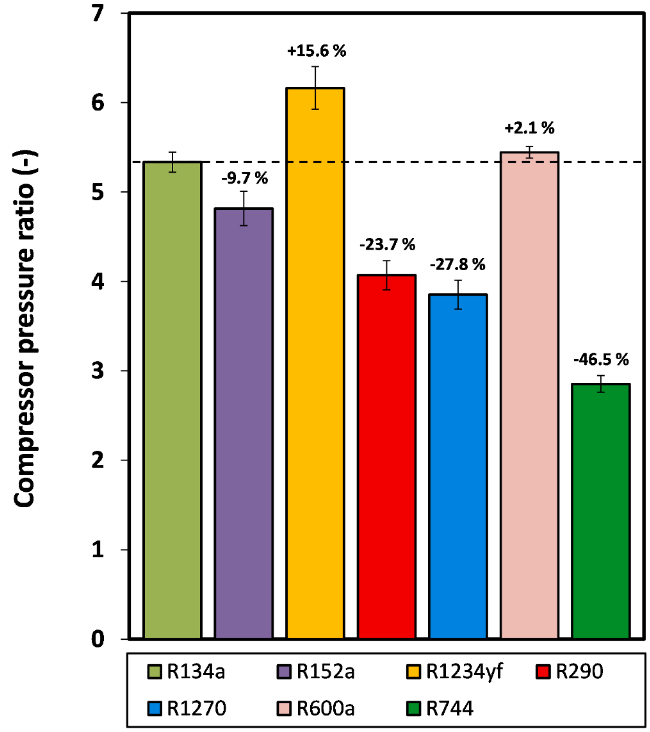

Fig. 10. Compressor pressure ratio.

lowest thermal capacity fluid, and the useful superheating is neglected to define the LMTD and the thermal efficiency at the evaporator. Figs. 11 and 12 present the results from these equations with a noticeable variability due to the dynamic operation of the refrigeration plant.

$$\varepsilon_{ihx} = \frac{T_{ihx\ lp\ out} - T_{ihx\ lp\ in}}{T_{ihx\ hp\ in} - T_{ihx\ lp\ in}} \tag{17}$$

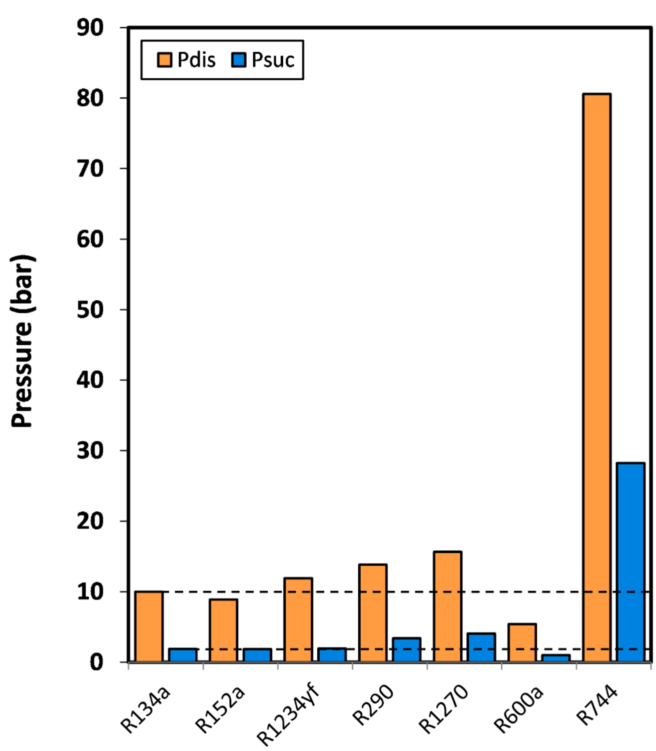

Fig. 9. Average compressor pressures (P_{suc}: suction pressure; P_{dis}: discharge pressure).

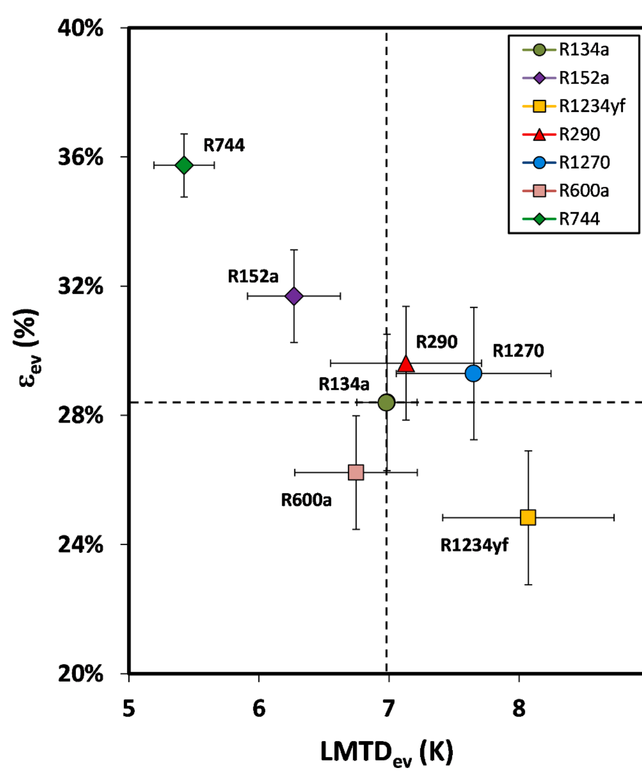

Fig. 11. Evaporator thermal efficiency vs. LMTD.

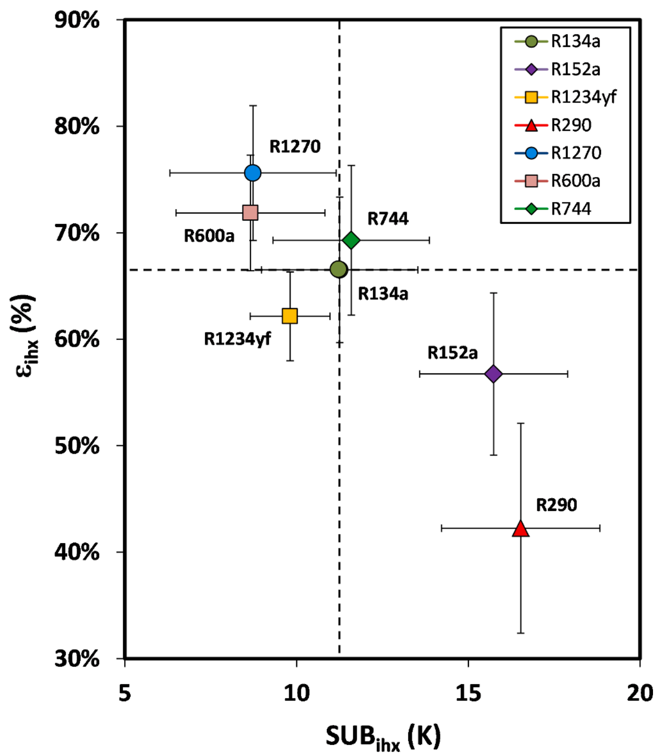

Fig. 12. IHX thermal efficiency vs. subcooling degree.

$$\varepsilon_{ev} = \frac{T_{ev\ air\ in} - T_{ev\ air\ out}}{T_{ev\ air\ in} - T_{ev}} \tag{18}$$

$$SUB_{ihx} = T_{ihx\ hp\ in} - T_{ihx\ hp\ out} \tag{19}$$

$$LMTD_{ev} = \frac{(T_{ev\ air\ in} - T_{ev\ air\ out})}{\ln\left(\frac{T_{ev\ air\ in} - T_{ev}}{T_{ev\ air\ out} - T_{ev}}\right)} \tag{20}$$

According to Fig. 11, the evaporator performs better with the refrigerants R744 and R152a because the value of the LMTD is lower than R134a and the thermal efficiency is higher. However, the opposite happens with the R1234yf, which has a slightly thermal efficiency but with higher LMTD than R134a. That agrees with the results presented in Fig. 7, where R1234yf gives a low evaporating temperature while the fluids R744 and R152a have a higher one. In addition, the hydrocarbons R290, R1270 and R600a results are similar to those from R134a, so we can affirm that the evaporator operates similar using hydrocarbons.

Regarding the IHX, Fig. 12 shows that the R744, the hydrocarbons R600a and R1270 and the HFO R1234yf present similar thermal efficiency values to R134a due to the high variability this parameter. Notwithstanding, hydrocarbons give higher values on average than R134a, which means that the IHX always perform better with this kind of refrigerant. On the other hand, the refrigerants R152a and R290 have lower values of thermal efficiency than R134a but higher subcooling degrees.

4.2.5. Pull-Down operation

The pull-down tests allow determining the time invested and the energy consumed by the beverage cooler to cool down the product from ambient conditions of 30 °C and 55% to the product target temperature (3.0 to 3.2 °C). For these tests, the refrigerant mass charge of the refrigerating unit is fixed to the optimal value determined previously. Fig. 13 shows the cooling process for all tested refrigerants and the energy consumption during the pull-down.

As Fig. 13 shows, there is no clear difference in the total time invested in the pull-down process, so it is difficult to affirm which is the quickest cooling refrigerant. Notwithstanding, it takes around 8 h to cool down the 15 probe cans, that is, near to the defrosting period set to the beverage cooler. Due to this, Table 9 summarizes the main parameters of the pull-down tests during 8 h, including the energy consumption depicted in Fig. 13, where it is evident that all tested refrigerants need less energy than R134a to reach the product target temperature starting at similar conditions. Special attention may be concern about the R152a with a reduction of −18.5%, and the hydrocarbons R290 and R1270 with a decrease of about −34.4% and −26.0%.

5. Conclusions

Based on the main idea of replacing the refrigerant R134a, this work experimentally analyses six low-GWP alternatives, including HFCs (R152a and R1234yf), hydrocarbons (R290, R1270 and R600a) and the inorganic substance carbon dioxide (R744). Using a beverage cooler as a

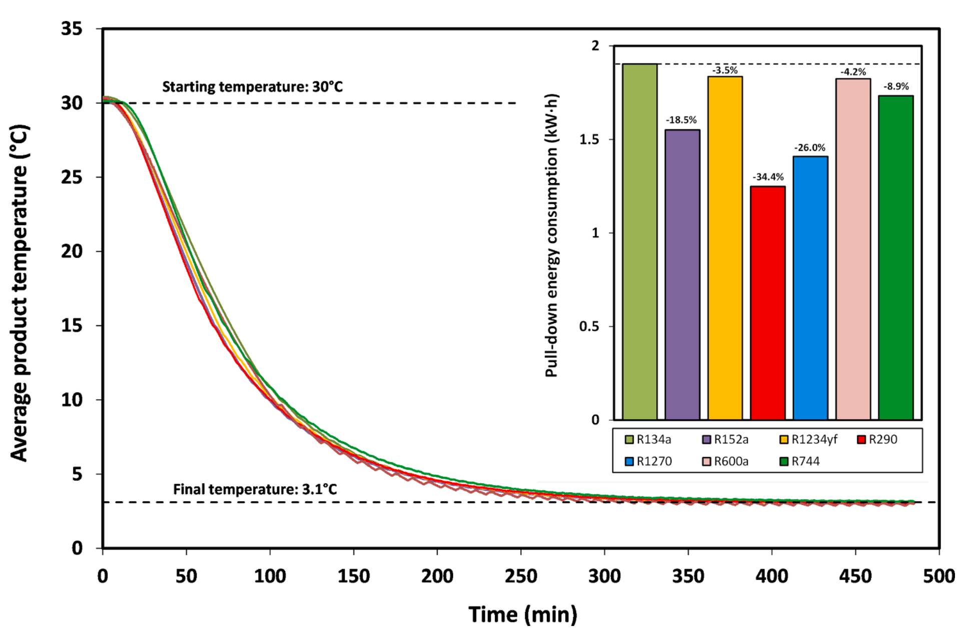

Fig. 13. Pull-down process and energy consumption.

Table 9
Main parameters during the pull-down process at the optimal mass charge.

Refrigerant	m_{opt} (g)	T_{env} (°C)	HR_{env} (%)	$T_{prod\ ini}$ (°C)	$T_{prod\ fin}$ (°C)	E_{8h} (kW·h)
R134a	242	30.3 ± 0.3	54.5 ± 1.8	30.4	3.0	1.90
R152a	246	30.1 ± 0.2	54.8 ± 1.6	30.0	3.1	1.55
R1234yf	271	30.0 ± 0.1	54.4 ± 0.3	30.2	3.0	1.84
R290	138	30.3 ± 0.2	53.0 ± 2.2	30.2	3.0	1.25
R1270	128	30.5 ± 0.2	52.8 ± 1.2	30.3	3.1	1.41
R600a	127	29.7 ± 0.1	54.6 ± 0.8	30.4	3.0	1.82
R744 (CO_2)	510	30.3 ± 0.5	53.9 ± 3.6	30.2	3.2	1.73

test bench, the analysis optimises the refrigerant mass charge to minimise the system's energy consumption by changing the compressor according to the fluid. From the results, the following main conclusions are underlined:

The use of hydrocarbons R290 and R1270 allows energy savings of −27.5% and −26.3%, respectively, followed by the HFC R152a (−13.7%), the inorganic R744 (−3.9%) and the hydrocarbon R600a (−1.2%). However, the HFO R1234yf penalises energy consumption up to 4.1%. The leading cause is the combination of the electrical power consumed by the system and the compressor running time, which is always higher for R600a and R1234yf.

The phase-change temperatures are very close to R134a, except R1234yf and R744. In the case of R1234yf, the condensing level remains higher, and the evaporating temperature is lower, responding to its low heat transfer performance. For R744, the gas-cooler exit temperature is almost similar to the ambient temperature due to the transcritical operation, and the evaporating level is higher.

The operating pressures depend on the phase-change temperatures, where R744 reports the highest values, followed by the hydrocarbons R1270 and R290 and the HFO R1234yf. The lowest working pressures correspond to the refrigerant R600a with pressure levels near to the atmospheric. Consequently, almost all refrigerants work with a lower pressure ratio than R134a, excluding R1234yf (15.6% higher) and R600 (2.1% higher). The carbon dioxide (R744) presents the lowest pressure ratio, reducing 46.5%, which positively affects the compressor's performance.

Regarding the heat exchangers, carbon dioxide (R744) reports higher values of thermal effectiveness in the evaporator (around 36%) and the IHX (close to 70%). The rest perform similar values to R134a for the evaporator, with some differences in the IHX for the fluids R152a and R290, which reach high subcooling degrees with relatively low thermal efficiency.

Finally, the pull-down process is more efficient for any of the tested fluids. Special mention goes to the hydrocarbons R290 and R1270, which energy savings are 34.4% and 26.0%, respectively.

CRediT authorship contribution statement

D. Sánchez: Investigation, Methodology, Writing – original draft. **A. Andreu-Nácher:** Data curation, Formal analysis. **D. Calleja-Anta:** Writing – review & editing. **R. Llopis:** Supervision. **R. Cabello:** Supervision.

Declaration of Competing Interest

The authors declare that they have no known competing financial interests or personal relationships that could have appeared to influence the work reported in this paper.

Acknowledgements

The authors gratefully acknowledge the financial support of the research projects from Ministerio de Ciencia, Tecnología y Telecomunicaciones in Spain (RTI2018-093501-B-C21), and the Jaume I University (UJI-B2019-56 and grant PREDOC/2019/19).

References

[1] Alsaad MA, Hammad MA. The application of propane/butane mixture for domestic refrigerators. Appl Therm Eng 1998;18:911–8.
[2] Aprea C, Greco A, Maiorino A. An experimental investigation on the substitution of HFC134a with HFO1234YF in a domestic refrigerator. Appl Therm Eng 2016;106:959–67.
[3] Aprea C, Greco A, Maiorino A, Masselli C, Metallo A. HFO1234ze as drop-in replacement for R134a in domestic refrigerators: an environmental impact analysis. Energy Procedia 2016;101:964–71.
[4] Aprea C, Greco A, Maiorino A. HFOs and their binary mixtures with HFC134a working as drop-in refrigerant in a household refrigerator: Energy analysis and environmental impact assessment. Appl Therm Eng 2018;141:226–33.
[5] ASHRAE, Handbook – Fundamentals (SI Edition) American Society of Heating, Refrigerating and Air Conditioning Engineers 2013 Englewood, Colorado (USA).
[6] Bell IH, Domanski PA, McLinden MO, Linteris GT. The hunt for nonflammable refrigerant blends to replace R-134a. Int. Journal of Refrigeration 2019;104:484–95.
[7] Belman-Flores JM, Rodríguez-Muñoz AP, Gutiérrez P-R, Mota-Babiloni A. Experimental study of R1234yf as a drop-in replacement for R134a in a domestic refrigerator. Int. Journal of Refrigeration 2017;81:1–11.
[8] Bitzer. *Refrigerant report 21*. A-501-21 EN (2020).
[9] Bobbo S, Nicola GD, Zilio C, Brown JS, Fedele L. Low GWP halocarbon refrigerants: A review of thermophysical properties. Int. Journal of Refrigeration 2018;90:181–201.
[10] Bolaji BO. Experimental study of R152a and R32 to replace R134a in a domestic refrigerator. Energy 2010;35:3793–8.
[11] Bolaji BO. Theoretical assessment of new low global warming potential refrigerant mixtures as eco-friendly alternatives in domestic refrigeration systems. Scientific African 2020;10:e00632. https://doi.org/10.1016/j.sciaf.2020.e00632.
[12] Cabello R, Sánchez D, Llopis R, Arauzo I, Torrella E. Experimental comparison between R152a and R134a working in a refrigeration facility equipped with a hermetic compressor. Int. Journal of Refrigeration 2015;60:92–105.
[13] Cabello R, Sánchez D, Llopis R, Torrella E. Experimental evaluation of the energy efficiency of a CO2 refrigerating plant working in transcritical conditions. Appl Therm Eng 2008;28(13):1596–604.
[14] Calm JM. The next generation of refrigerants – Historical review, considerations, and outlook. Int. Journal of Refrigeration 2008;31(7):1123–33.
[15] Cecchinato L, Corradi M. Transcritical carbon dioxide small commercial cooling applications analysis. Int. Journal of Refrigeration 2011;34:50–62.
[16] DeAngelis JM, Hrnjak PS. *Experimental study of system performance improvements in transcritical R744 systems with applications to bottle coolers*. ACRC CR-57. University of Illinois; 2005.
[17] Elbel S, Padilla FY, Bowers C, Hrnjak P. Successful conversion and validation of glass door merchandisers using transcritical R744. 11th IIR Gustav Lorentzen Conference on Natural Refrigerants. 2014.
[18] Elbel S, Visek M, Hrnjak PS. A fair comparison of CO_2 and Propane used in light commercial applications featuring natural refrigerants. International Refrigeration and Air Conditioning Conference. 2016.
[19] EPA. Transitioning to low-GWP alternatives in commercial refrigeration. USA Environmental Protection Agency 2016.
[20] Fatouh M, El Kafafy M. Assessment of propane/commercial butane mixtures as possible alternatives to R134a in domestic refrigerators. Energy Convers Manage 2006;47(15-16):2644–58.
[21] Fatouh M, Kafafy ME. Experimental evaluation of a domestic refrigerator working with LPG. Appl Therm Eng 2006;26(14-15):1593–603.
[22] Granryd E. Hydrocarbons as refrigerants - an overview. Int. Journal of Refrigeration 2001;24:15–24.
[23] Hammad MA, Alsaad MA. The use of hydrocarbons mixtures as refrigerants in domestic refrigerators. Appl Therm Eng 1999;19:1181–9.
[24] IIR. *Refrigerant charge reduction in refrigerating systems.* 25th Informatory Note on Refrigeration Technologies. May (2014).
[25] IIR Harmonization of Life Cycle Climate Performance Methodology 32th Informatory Note on Refrigeration Technologies October (2016).
[26] IIR. *The role of refrigeration in the global economy.* 38th Informatory Note on Refrigeration Technologies. June (2019).
[27] Illán-Gómez F, López-Belchí A, García-Cascales JR, Vera-García F. Experimental two-phase heat transfer coefficient and frictional pressure drop inside mini-channels during condensation with R1234yf and R134a. Int. Journal of Refrigeration 2015;51:12–23.
[28] IPCC Special Report: Safeguarding the Ozone Layer and the Global Climate System. Chapter 2005 4.
[29] IPCC. *Climate Change 2007: The Physical Science Basis. Contribution of Working Group I to the 4th Assessment Report of the Intergovernmental Panel on Climate Change* in: Press, Cambridge University Press: New York, USA (2007).

[30] IPCC. Climate Change 2013: The Physical Science Basis. Contribution of Working Group I to the 5th Assessment Report of the Intergovernmental Panel on Climate Change. 1st ed.;. New York, USA: Cambridge University Press; 2013.
[31] IPCC. *Climate Change 2021: The Physical Science Basis. Contribution of Working Group I to the 6th Assessment Report of the Intergovernmental Panel on Climate Change* in: Press, Cambridge University Press: New York, USA (2021).
[32] B. Jacob A. Azar P. Nekså Performance of CO2-refrigeration (R-744) in commercial cold drink equipment 2006 Trondheim, Norway, May 28 31.
[33] Jung D, Kim C, Song K, Park B. Testing of propane/isobutane mixture in domestic refrigerators. Int. Journal of Refrigeration 2000;23:517–27.
[34] Jwo C, Ting C, Wang W. Efficiency analysis of home refrigerators by replacing hydrocarbon refrigerants. Measurement 2009;42:697–701.
[35] Karber KM, Abdelaziz O, Vineyard EA. Experimental Performance of R-1234yf as a Drop-in Replacement for R-134a in Domestic Refrigerators. International Refrigeration and Air Conditioning Conference. 2012.
[36] Lee YS, Su CC. Experimental studies of isobutane (R600a) as the refrigerant in domestic refrigeration system. Appl Therm Eng 2002;22:507–19.
[37] Lee M, Lee D, Kim Y. Performance characteristics of a small-capacity directly cooled refrigerator using R290/R600a (55/45). Int. Journal of Refrigeration 2008; 31:734–41.
[38] Lemmon E.W., Huber M.L., McLinden M.O., *Reference fluid thermodynamic and transport properties (REFPROP)*, NIST Standard Reference Database 23, v.10.0. National Institute of Standards, Gaithersburg MD, USA (2018).
[39] Maiorino A, Aprea C, Del Duca MG, Llopis R, Sánchez D, Cabello R. R-152a as an alternative refrigerant to R-134a in domestic refrigerators: An experimental analysis. Int. Journal of Refrigeration 2018;96:106–16.
[40] Minor B, Montoya C, Kasa FS. HFO-1234yf Performance in a Beverage Cooler. International Refrigeration and Air Conditioning Conference. 2010.
[41] Mohanraj M, Jayaraj S, Muraleedharan C, Chandrasekar P. Experimental investigation of R290/R600a mixture as an alternative to R134a in a domestic refrigerator. Int. Journal of Thermal Sciences 2009;48:1036–42.
[42] Mohanraj M, Jayaraj S, Muraleedharan C. Environment friendly alternatives to halogenated refrigerants—A review. Int. Journal of Greenhouse Gas Control 2009; 3(1):108–19.
[43] Mohanraj M. Energy performance assessment of R430A as a possible alternative refrigerant to R134a in domestic refrigerators. Energy for Suitable Development 2013;17:471–6.
[44] Morales-Fuentes A, Ramírez-Hernández HG, Méndez-Díaz S, Martínez-Martínez S, Sánchez-Cruz FA, Silva-Romero JC, et al. Experimental study on the operating characteristics of a display refrigerator phasing out R134a to R1234yf. Int. Journal of Refrigeration 2021;130:317–29.
[45] Nair V. HFO refrigerants: A review of present status and future prospects. Int. Journal of Refrigeration 2021;122:156–70.
[46] Padilla FY, Hrnjak P, Elbel S, High-efficiency. low-cost glass door merchandisers using transcritical Carbon Dioxide. 24th IIR International Congress of Refrigeration. 2015.
[47] Park KJ, Jung D. Performance of alternative refrigerant R430A on domestic water purifiers. Energy Convers Manage 2009;50:3045–50.
[48] Poggi F, Macchi-Tejada H, Leducq D, Bontemps A. Refrigerant charge in refrigerating systems and strategies of charge reduction. Int. Journal of Refrigeration 2008;31:353–70.
[49] Rasti M, Aghamiri S, Hatamipour M. Energy efficiency enhancement of a domestic refrigerator using R436A and R600a as alternative refrigerants to R134a. Int. Journal of Thermal Sciences 2013;74:86–94.
[50] C. Rohrer Transcritical, CO2 bottle cooler development. 7th IIR Gustav Lorentzen Conference on Natural Working Fluids 2006 Trondheim, Norway, May 28 31.
[51] Roy Zunipa, Halder Gopinath. Replacement of halogenated refrigerants towards sustainable cooling system: A review. Chemical Engineering Journal Advances 2020;3:100027. https://doi.org/10.1016/j.ceja.2020.100027.
[52] Sánchez D, Cabello R, Llopis R, Arauzo I, Catalán-Gil J, Torrella E. Energy performance evaluation of R1234yf, R1234ze(E), R600a, R290 and R152a as low-GWP R134a alternatives. Int. Journal of Refrigeration 2017;74:269–82.
[53] Sánchez D, Catalán-Gil J, Cabello R, Calleja-Anta D, Llopis R, Nebot-Andrés L. Experimental analysis and optimization of an R744 Transcritical cycle working with a mechanical subcooling system. Energies 2020;13:3204.
[54] Sattar MA, Saidur R, Masjuki HH, Butane. isobutane and their mixtures as an alternatives to R-134a in domestic refrigerator. Int. Journal of Mechanical and Materials Engineering 2 2007;n° 2:154–60.
[55] Shapiro D. Drop-in Testing of Next-Generation R134a Alternates in a Commercial Bottle Cooler/Freezer. International Refrigeration and Air Conditioning Conference. 2012.
[56] Torrella E, Sánchez D, Llopis R, Cabello R. Energetic evaluation of an internal heat exchanger in a CO_2 transcritical refrigeration plant using experimental data. Int. Journal of Refrigeration 2011;34(1):40–9.
[57] Visek M, Elbel S, Hrnjak PS. Conversion of cold beverage dispenser's refrigeration system to R744 refrigerant. International Refrigeration and Air Conditioning Conference. 2016.
[58] Wongwises Somchai, Chimres Nares. Experimental study of hydrocarbon mixtures to replace HFC-134a in a domestic refrigerator. Energy Convers Manage 2005;46 (1):85–100.
[59] Yana Motta SF, Vera Bercerra ED, Spatz MW. Analysis of LGWP Alternatives for Small Refrigeration (Plugin) Applications. International Refrigeration and Air Conditioning Conference. 2010.
[60] Yu Chao-Chieh, Teng Tun-Ping. Retrofit assessment of refrigerator using hydrocarbon refrigerants. Appl Therm Eng 2014;66(1-2):507–18.